Simultaneous imaging of hyperpolarized [1,4-13 C2]fumarate, [1-13 C]pyruvate and 18 F-FDG in a rat model of necrosis in a clinical PET/MR scanner

Eldirdiri, Abubakr; Clemmensen, Andreas; Bowen, Sean; Kjær, Andreas ; Ardenkjær-Larsen, Jan Henrik

Published in:
N M R in Biomedicine

Link to article, DOI:
10.1002/nbm.3803

Publication date:
2017

Document Version
Peer reviewed version

Simultaneous imaging of hyperpolarized [1,4-$^{13}C_2$]fumarate, [1-^{13}C]pyruvate and ^{18}F-FDG in rat model of necrosis in a clinical PET/MR

Abubakr Eldirdiri[1, 3,*], Andreas Clemmensen[3, 4, 5,*], Sean Bowen[1], Andreas Kjær[4, 5], Jan Henrik Ardenkjær-Larsen[1, 2, ¥]

1. Department of Electrical Engineering, Technical University of Denmark, Kgs. Lyngby, Denmark
2. GE Healthcare, Broendby, Denmark
3. Danish Research Center for Magnetic Resonance, Copenhagen University Hospital Hvidovre, Denmark
4. Department of Clinical Physiology, Nuclear Medicine and PET, Rigshospitalet, Copenhagen, Denmark
5. Cluster for Molecular Imaging, Department of Biomedical Medical Sciences, University of Copenhagen, Denmark

* These authors contributed equally to this work.

¥ Corresponding author: Jan H. Ardenkjaer-Larsen, Ph.D., Technical University of Denmark, Orsted Plads 375/148, 2800 Kgs Lyngby, Denmark, jhar@elektro.dtu.dk

Word count: 5411

Keywords: Hyperpolarization; [1-^{13}C]pyruvate; [1,4-$^{13}C_2$]fumarate, ^{18}F-FDG, PET/MR

Abbreviations: dDNP: dissolution Dynamic Nuclear Polarization, PA: [1-^{13}C]pyruvate, FA: [1,4-$^{13}C_2$]fumarate, FDG: 2-fluoro-2-deoxy-D-glucose, PET: Positron Emission Tomography, DM: dissolution medium, NM: neutralizing medium, LN_2: liquid nitrogen

Abstract

A co-polarization scheme for [1,4-$^{13}C_2$]fumarate and [1-^{13}C]pyruvate is presented to simultaneously assess necrosis and metabolism in rats with hyperpolarized ^{13}C MR. The co-polarization was performed in a SPINlab polarizer. In addition, the feasibility of simultaneous PET and MR of small animals with a clinical PET/MR is demonstrated. The hyperpolarized metabolic MR and PET is demonstrated in a rat model of necrosis.

The polarization and T_1 of the co-polarized [1,4-$^{13}C_2$]fumarate and [1-^{13}C]pyruvate substrates were measured *in vitro* and compared to those obtained when the substrates were polarized individually. A polarization of 36±4 % for fumarate and 37±6% for pyruvate was obtained. We found no significant difference in the polarization and T_1 values between the dual and single substrate polarization.

Rats weighing about 400 g were injected i.m. in one of the hind legs with 200 µL of turpentine to induce necrosis. Two hours later, ^{13}C metabolic maps were obtained with a Chemical Shift Imaging sequence (16x16) with a resolution of 3.1x5.0x25.0 mm^3. The ^{13}C spectroscopic images were acquired in 12 s, followed by an 8 min ^{18}F-FDG PET acquisition of 3.5 mm resolution. [1,4-$^{13}C_2$]malate was observed from the tissue injected with turpentine indicating necrosis. Normal [1-^{13}C]pyruvate metabolism and ^{18}F-FDG uptake were observed from the same tissue.

The proposed co-polarization scheme provides a means to utilize multiple imaging agents simultaneously, and thus to probe various metabolic pathways in a single examination. Moreover, it demonstrates the feasibility of small animal research on a clinical PET/MR scanner for combined PET and hyperpolarized metabolic MR.

Introduction

Since the introduction of the dissolution Dynamic Nuclear Polarization (dDNP) technique[1] to enhance the ^{13}C signal in applications like magnetic resonance spectroscopic imaging (MRSI), the metabolic fluxes of hyperpolarized ^{13}C substrates have shown great potential to improve the detection and characterization of many pathologies, especially cancer. For instance, studies have indicated that the lactate signal [2-4], and in some cancer types the alanine signal [5], are higher in cancer than in normal tissue, after the administration of hyperpolarized [1-^{13}C]pyruvate. This observation is referred to as the Warburg effect and it is due to the fact that most cancer cells have elevated glycolysis even in the presence of sufficient oxygen. Moreover, MR imaging with hyperpolarized [1,4-$^{13}C_2$]fumarate was shown to allow early detection of necrosis [6-8]. The conversion of fumarate into malate is a normal step in the mitochondrial tricarboxylic acid cycle and is catalyzed by fumarase. As the enzyme is not present in the extracellular space, but exposed by cells that undergo necrosis, it is demonstrated that the observation of an increased [1,4-$^{13}C_2$]malate production, after intravenous administration of hyperpolarized [1,4-$^{13}C_2$]fumarate, can be used as a marker of necrosis.

In order for the DNP process to be effective, it is important to comply with certain requirements during sample preparation and polarization. First of all, the ^{13}C labeled substrates must be in an amorphous (glassy) solid state with the appropriate electron paramagnetic agent uniformly distributed, such that an efficient coupling between electron spin and nuclear spins is achieved in the solid state [1,9,10]. Fumaric acid (FA) dissolved in dimethyl sulfoxide, for instance, requires rapid freezing to achieve this amorphous solid state and to prevent the FA crystallization, which can significantly reduce the nuclear spin

polarization. Pyruvic acid (PA), on the other hand, is a liquid at room temperature that glasses well without additives. Moreover, the concentration of the desired agents, solvent/glassing agents and the concentration and type of free radical must all be optimized to achieve optimal polarization for the ^{13}C substrates. In addition, appropriate dissolution medium (DM) and neutralizing medium (NM) must be prepared for each agent in order to ensure physiological pH and osmolarity/tonicity for *in vivo* use.

The spectrum obtained following the *in vivo* infusion of a hyperpolarized ^{13}C material is often sparse. In some cases, this sparsity can be exploited to combine more than one ^{13}C agent during the hyperpolarization and imaging. This way multiple enzymatic pathways can be probed simultaneously. Previous attempts of multi-agent polarization have been performed with the Hypersense (Oxford Instruments, UK) polarizer [11-14]. This study presents a co-polarization scheme for [1,4-$^{13}C_2$]fumarate and [1-^{13}C]pyruvate to simultaneously assess necrosis and metabolism. The co-polarization presented in this work is performed in a SPINlab polarizer (GE Healthcare) [15,16]. Although the SPINlab benefits from relatively higher magnetic field and lower temperature, which result in high polarization, the polarization build-up durations are considerably longer (2~4 hours). The SPINlab overcomes this in part by having four samples in parallel; however, the adoption of multi-substrate polarization scheme makes the polarization in SPINlab more appealing. The polarization and T_1 of the co-polarized [1,4-$^{13}C_2$]fumarate and [1-^{13}C]pyruvate were measured in phantoms and compared to those obtained when the substrates were polarized individually. *In vivo* experiments were conducted in rats with induced necrosis via the injection of 200 µL of turpentine at the deep muscle of the left hind leg. ^{13}C metabolic maps were obtained to assess the cellular uptake and the conversion of [1-

^{13}C]pyruvate into [1-^{13}C]lactate and to assess the conversion of [1,4-$^{13}C_2$]fumarate into [1,4-$^{13}C_2$]malate. In addition, ^{18}F-fluorodeoxyglucose (^{18}F-FDG) Positron Emission Tomography (PET) images were acquired simultaneously with the ^{13}C MRSI.

Experimental

Sample preparation

For pyruvate preparation, AH111501 trityl radical (GE Healthcare, Denmark) was added to a sample of [1-^{13}C]pyruvic acid (PA) (14 M) (Sigma Aldrich, Denmark) to a final concentration of 15 mM. The fumarate was prepared by dissolving [1,4-$^{13}C_2$]fumaric acid (FA) (Cambridge Isotope Laboratories, MA, USA) in dimethyl sulfoxide (DMSO) (Sigma Aldrich, Denmark). Sonication and vortex mixing were used until all the FA crystals had dissolved. AH111051 radical was then added and dissolved in the solution. To optimize the formulation of FA, three different batches were prepared with FA/radical concentrations of 3.6 M/8 mM, 3.6 M/12 mM and 2.8 M/15 mM, respectively.

The polarizer and fluid path assembly

The co-polarization was made in a SPINlab polarizer (GE Healthcare, Denmark). Figure 1-a shows the fluid path assembly designed for use with the SPINlab. The fluid path consists of a vial (1) containing the sample and connected to the dissolution syringe (2) via two concentric tubes (3). The tubes can be pushed into the polarizer through the dynamic seal (4) without compromising the vacuum. The syringe has an exit port (5) that connects to a tube for transfer of the hyperpolarized solution.

115 The regular sample preparation procedure for the SPINlab fluid path requires that the vial,
116 after adding the ^{13}C substrate, is frozen in liquid nitrogen (LN_2). This freezing is necessary
117 to perform pressure check and helium purging. Helium purging is needed to have a helium
118 exchange gas inside the fluid path when the vial is cooled to <1 K.

119 The regular procedure to load the sample into the SPINlab involves lowering the sample
120 vial into the sample pot (see Figure 1-c), were the hyperpolarization take place, through
121 multiple steps (gradual insertion over 15 min) to avoid excessive increase in the helium
122 temperature. This multi-steps lowering process was found to result in FA crystallization.
123 Therefore, to avoid the FA crystallization, the sample preparation and loading was
124 modified as detailed in the next section.

125 **Co-polarization of FA and PA**

126 The fluid path was prepared by first placing 25 µL (around 350 µmol) of PA in the sample
127 vial and then freezing it in LN_2. 100 µL (about 350 µmol) of FA was then added on top of
128 the PA and the vial was placed in LN_2 again (see Figure 1-b). The vial is then glued to the
129 tube set with the tip immersed in LN2 and the neck above the liquid surface. The rest of
130 the fluid path preparations (pressure check and He purging) were done according to the
131 manufactures instructions. After the preparation, the fluid path was placed in the SPINlab
132 and the vial containing the two compounds was initially placed at the airlock for 20 to 30
133 min, thus allowing the substrates to thaw before lowering the sample vial into the helium
134 pot. During the melting period, it is assumed that the difference in density prevents the
135 mixing of the two substrates. The densities of PA and FA solutions are 1.3 g/mL and 1.2
136 g/mL, respectively. Then the sample vial was directly lowered into the helium bath in either
137 one (A: directly to the sample pot) or two steps (B: directly to the sample pot and then

retracted to the 4 K thermal link for 10 min), instead of the normal scheme of going through a multi-step lowering process, to avoid the crystallization of the FA in the sample.

For both *in vivo* and *in vitro* studies, the sample was irradiated with microwaves at 139.64 GHz and 40 mW (the two samples have the same optimal microwave frequency). The sample was polarized for at least 4 h in the *in vitro* phantom studies to measure the liquid-state polarization. Before dissolving the samples, it was ensured that the polarization curve in the SPINlab reached the flat plateau. In the *in vivo* animal experiments the samples were polarized for about 3 h, i.e. after reaching more than 90% of maximum. The polarization curve was fitted with a single exponential.

The dissolution syringe was filled with about 15 g of a DM (water for injection with 0.1 g/L ethylenediaminetetraacetic acid disodium salt dehydrate). The dissolved sample was mixed with 0.95 g of NM (water for injection with 0.72 M NaOH, 0.4 M 2-Amino-2-(hydroxymethyl)-1,3-propanediol and 0.1 g/L ethylenediaminetetraacetic acid disodium salt dehydrate).

Some of the dissolved samples were used after the *in vitro* study to measure the concentration of the two substrates. The concertation was measured by quantitative NMR using a 400 MHz spectrometer (DirectDrive, Agilent) and a 100 mM ^{13}C-urea reference.

Single substrate polarization

In addition to the dual polarization of FA and PA, the FA was polarized separately. This was to investigate if there are differences in T_1 and polarization values between the single and dual substrate polarization. The single FA polarization and dissolution was made in the same manner as described in the previous section for the dual substrate. About 350

μmol (100 μL) of FA sample was loaded in the vial and dissolved with 15 g of DM and 0.65 g of NM.

Phantom MR experiments for polarization and T_1 measurements

All imaging was performed in a clinical 3T PET/MR scanner (Siemens mMR Biograph, Siemens, Erlangen, Germany). A dual-tuned transmit/receive flex surface coil (RAPID Biomedical) was used for both ^{1}H and ^{13}C acquisition. The coil consists of a 110 mm loop for ^{13}C and a 180 mm x 244 mm butterfly for ^{1}H. The 90° flip angle was calibrated from a ^{13}C-urea phantom at approximately the position of the rat. Phantoms and rats were placed in the center of the 11 cm loop coil.

About 5 mL of the polarized material was injected into a previously shimmed phantom tube, approximately 30 s after the dissolution. 180 ^{13}C spectra were acquired without spatial encoding using an excitation pulse with 5° flip angle (315 us pulse duration) and repetition time TR of 5 s. The sampling spectral window was set to 6000 Hz with 512 spectral points.

For each spectrum of the dynamic acquisition, the signal integrals were calculated after baseline correction. A mono-exponential decay function, equation 1, was fitted for each of the two substrate signals to obtain the relaxation time, T_1, and the initial longitudinal magnetization, M_I.

$$S(n) \propto M_I \, sin(\alpha) \cos^n(\alpha) \, e^{-n\frac{TR}{T1}} \qquad (1),$$

where $S(n)$ is the signal recorded after the nth excitations, TR is the repetition time, and α is the flip angle.

A ^{13}C-urea phantom (4 M) was placed next to the tube with the hyperpolarized solution and was used to calibrate the 90^{o} flip angle and as a reference to measure the polarization. To quantify the polarization, the initial signal of the hyperpolarized sample was compared to the urea signal and corrected for the concentration difference.

In vivo rat experiment

Animal handling and experimental procedures were performed according to the guidelines from Danish Animal Experiments Inspectorate (permit no. 2011/561−14). The *in vivo* study was conducted in two rats weighing (400 g). The first rat was only injected with hyperpolarized FA. The second rat received two injections separated by 10 min. The first injection was only hyperpolarized FA, and the second injection was dual polarized FA and PA. Necrosis was induced by intramuscular injection of 200 µL of sterile turpentine oil in one of the hind legs. This was followed by subcutaneous injection of 400 µL of Buprenorphine (TEMGESIC, 0.03 mg/mL) to control the acute paint from the turpentine injection. Two hours later, the animal was transferred to the PET/MR scanner to acquire ^{13}C MRS and PET images.

During the MR scanning, the animals were anaesthetized with 3% Sevoflurane mixed in O_2. A catheter was inserted in the tail vein for the administration of the hyperpolarized mixture of pyruvate and fumarate or fumarate alone. 2 mL (0.14 mmol/kg) of the co-polarized substrates was injected in the rat. This injection was done approximately 20 s after dissolution, during this period the co-polarized material was transferred to the MRI room from the SPINlab in a syringe that was then connected to the tail vein catheter. The hyperpolarized substrate was injected manually over a period of 10 s.

Anatomical long axis proton MR images were acquired prior to the ^{13}C MRS scans for spatial localization of the necrotic tissue within muscle. Chemical shift images (CSI) (with FA=10°, TR= 80 ms, TE = 1.4 ms, FOV = 50 x 80 mm^2, matrix=16x16, nominal in-plane resolution 3.1 x 5 mm^2, slice thickness = 25 mm) were acquired 20 s after the end of administration of the hyperpolarised [1-^{13}C]pyruvate and [1,4-$^{13}C_2$]fumarate mixture.

One hour before the PET/MR imaging session, the rats were intravenously injected with 80 MBq of ^{18}F-FDG. An 8 min PET scan (3.5 mm isotropic resolution) was acquired during the acquisition of the MR images. Dixon imaging was used to obtain fat and water maps that were used to correct for the attenuation in the PET images.

The acquired free induction decay signal at each voxel of the CSI data was first zero-filled by a factor two to increase the spectral resolution, and the signal was then apodized using an exponential function, $e^{-f.t}$ with $f = 15\ \mathrm{Hz}$. Metabolic maps were generated for each metabolite from the peak amplitude in the real phased spectra after baseline correction and fitting with a generalized linear model. The metabolic maps were resampled to the same resolution of the anatomical proton images, 0.4x0.4 mm^2, and registered onto them. Thresholding was applied to remove the noise level. The metabolite maps were normalized with respect to the standard deviation of the noise, which was estimated from a background region outside of the animal.

Results

Polarization of [1,4-$^{13}C_2$]fumarate and [1-^{13}C]pyruvate

Figure 2 shows representative polarization build-up and the temperature curves recorded at the equilibrator and sample pot for the multi-step lowering process, typically used for PA, and the two-step lowering process, used for samples containing FA. The efficiency of the multi-step lowering process in minimizing the temperature variation at the sample pot is evident.

The polarization of samples containing 600 mg of FA from the three different batches (with FA/AH111051 concentrations of 2.8M/15mM, 3.6M/8mM and 3.6M/12mM) resulted in build-up time constants and final solid-state polarization values detailed in Table 1, for one and two insertion steps. The batches showed high variation in build-up time constant and less variation in the saturation level. The batch with 3.6M/12mM FA/AH111051 concentration had the shortest build-up time constant. This batch also showed no significant difference between the one (A) and two (B) lowering steps in the final saturation level, but the build-up time constant was shorter for (A) ; however, the one-step lowering can result in a higher increase in the sample pot temperature. The final solid state polarization values for these batches were comparable. The solid state NMR signals may vary significantly between measurements due to the uncontrolled position of the sample within the NMR coil that is dimensioned to hold up to four samples. However, the comparison is based on the liquid state polarization obtained post dissolution.

Table 1 also shows the liquid state polarization measurements obtained for the three formulations of fumarate via dynamic acquisition of ^{13}C spectra in the PET/MR scanner

30 s after dissolution. There was no difference between the batches in the measured polarization. Since all the batches gave similar polarization results, the subsequent experiments were conducted with the 3.6M/12mM FA/AH111051 batch. This batch gives higher concentration of fumarate, which results in higher MR signal. In addition, this batch had relatively faster polarization build-up.

The results of the experiment to determine whether there is a difference in the polarization and T_1 values between the dual and single substrate polarization is summarized in Table 2. No significant difference was found in the measured values of polarization of FA for single and dual FA/PA polarization. The polarization level of PA, 37%, obtained with the dual polarization scheme agrees with the polarization values found in the literature [17].

After the dissolution of the polarized materials in the (15 g) DM and (0.95 g) NM, the measured concentrations of fumarate and pyruvate were about 31±2 mM (n=2). The measured pH value was 7.7±0.3 (n=8). The volume of the sample received after dissolution was 6±1 mL (n=3). The remaining volume was retained in the fluid path during the dissolution as dead volume.

Animal experiment

Figure 3 shows the expected position of the metabolite peaks. The spectrum is sparse enough to allow clear quantification the injected substrates and their products. Figure 4 shows the anatomical image and the ^{13}C spectrum at the necrotic tissue for the rat that was injected with only hyperpolarized fumarate. The maps of fumarate and malate distributions within a slice covering the necrotic region, in addition to FDG-PET, are also shown in Figure 4. Figure 5, shows the anatomical image and the ^{13}C spectrum at the

necrotic tissue for the rat that received the dually hyperpolarized fumarate and pyruvate. Clear malate signal was visible at the necrotic site with both the single fumarate and dual pyruvate/fumarate injections and no malate signal was observed elsewhere. Figure 5 also shows the PET images acquired for the same animal during the same MR imaging session. The FDG uptake by the different organs is represented using maximum intensity projection. An increase in the signal from lactate and from other pyruvate products was observed at the necrotic tissue. There is no clear effect from the necrosis on the FDG-PET signature.

Discussion

The main aim of this study was to investigate the technical feasibility of a method to simultaneously polarize a low dose of FA and PA in a SPINlab polarizer, and to image their metabolism in small animals with a clinical MR scanner. This setup provides a mean to utilize multiple imaging agents at once, and thus to probe various physiological characteristics and obtain valuable biological data, in a single examination. Secondly, it enables small animal research on a typical clinical scanner setup. Increased conversion of pyruvate into lactate, also known as the Warburg effect, is a main hallmark of neoplastic activity [18] and has the potential to effectively monitor the response to treatment [19]. The production of malate from fumarate has been proposed as sign for necrosis [6,8,20], and it is expected that the degree of necrosis induced by treatment, is proportional to the amount of malate produced. The amount of malate observed in the ^{13}C spectrum depends also on the time of imaging following the intervention as seen in the difference in malate

signal between the two injections in rat two. This is because the fumarase is washed out of the tissue within a few hours to the blood plasma and then to the urine [21].

High lactate signal, and also high signal from other pyruvate products like alanine and bicarbonate, was also observed at the necrotic muscle tissue in the *in vivo* experiment with dual FA and PA injection. The increased signal from pyruvate products is not unexpected, since intracellular enzymes like LDH also escape to the extracellular space when the cellular membranes are broken [22]. This is important to bear in mind, since many types of therapies induce necrosis in cancer tissue, which may result in elevated lactate production after injection of hyperpolarized pyruvate. Moreover, there is also evidence that cancer cells that survive the treatment, can benefit from the inflammatory response that follows, since it promote proliferation by providing the tumor environment with growth factors, survival factors and proangiogenic factors [23,24]. Therefore, simultaneous assessment of metabolism and necrosis with the setup proposed here can give a more complete picture, and allow distinguishing whether the high lactate signal is because the necrosis process from therapy is taking effect or because the tumor is thriving. Another factor contributing to the higher signal from pyruvate and its metabolites in this model, could be a higher cellular uptake of pyruvate. In any case, the appearance of the malate signal is a much more sensitive marker of necrosis than a small change in the large lactate signal.

Acquiring PET images at the same time as ^{13}C hyperpolarized MR imaging adds additional molecular imaging characterization, and allows comparing PET tracers with their analogous MR counterparts. For instance, although ^{18}F-FDG, unlike [1-^{13}C]pyruvate, does not show the actual metabolic reactions, the concentrations of ^{18}F-FDG in the PET

images reflects regional uptake of glucose. Thus, FDG-PET also reflects tissues with high metabolic activity, and the two markers, ^{18}F-FDG and ^{13}C-pyruvate, can be complementary [25,26]. The lactate signal was clearly detectable at various tissues from the ^{13}C spectra of the CSI whereas the malate signal was confined to necrotic tissue. There was no change in the FDG uptake or the lactate signal.

We were able to demonstrate the feasibility of using a state-of-the-art clinical PET/MR scanner for *in vivo* imaging of rats. Good image quality that allows the evaluation of metabolic activities in various tissues was achievable with both PET and ^{13}C-MRS imaging. In this study, the in-plane resolution used with CSI was 3.1 x 5 mm^2, but finer spatial resolution can be achieved. The minimal in-plane resolution for the CSI allowed on our system is 3.1 mm with nominal gradient strength, which is the maximum value that the manufacturer recommends for reliable performance. However, in theory, a resolution as fine as 1.5 mm can be achieved with the maximum gradient strength that can be realized by the scanner. This is because, the CSI sequence does not require very strong gradients, unlike other faster spectroscopic sequences, such as Echo Planar Spectroscopic Imaging (EPSI), which can be very demanding on gradient strength and slew rate. The maximum gradient strengths and slew rate on the Siemens mMR Biograph are 42 mT/m and 180 mT/m/ms, respectively. These are significantly lower compared to 1,000 mT/m gradient strength and 5,000 mT/m/ms slew rates on some of the state-of-the-art animal scanners.

One of the major problems that faced previous attempts of multi substrate polarization was the limited sample volume that can be polarized stably and dissolved successfully in the Hypersense polarizer (Oxfords, Instruments, UK), which is used in these co-

polarization attempts. The limited sample volume that can be used in the Hypersense subsequently results in relatively smaller concentrations of the co-polarized substrates in the final volume (13). SPINlab on the other hand is designed to efficiently polarize and dissolve larger substrate volumes (up to 2 g).

Relatively high polarization was achieved for both FA and PA (more than 30%) when they were polarized simultaneously in the SPINlab. In addition, there was no significant difference in the polarization and T_1 measurement compared to when the two substrates were polarized separately. The final concentration of the two agents after dissolution was acceptable for *in vivo* experiments (30 mM). This concentration however can be increased by increasing the initial volume of PA and FA in the sample vial, but will be at the expense of a larger waste. The dissolution volume can also be lowered for higher final concentration of PA and FA. The minimal effective dissolution volume that can be reliably used on the SPINlab is approximately 5-7 mL.

Using multiple ^{13}C substrates, however, brings additional burden to resolve multiple peaks in the frequency spectrum with the possibility of overlap between peaks; an issue which is less common in hyperpolarized ^{13}C MRS compared to ^{1}H MRS. Higher magnetic fields are more suitable for such tasks, since they give larger spacing between the peaks. Fortunately, the malate doublet was quantifiable in both single fumarate and dual fumarate/pyruvate scheme. There is also the problem of the difference in the optimal microwave irradiation frequencies for the different ^{13}C substrates, which can limit the solid state polarization for some of them. In our case, both FA and PA had the same optimal microwave frequency.

Necrosis has been shown to play an important role in many pathological processes like central nervous system and neurodegenerative disorders [27,28], ischemia/reperfusion injuries [21], viral and microbial infections [29,30]. Necrosis may also play an important role in physiological processes like ovulation [31] and embryogenesis [32]. In addition, many chemotherapeutical agents used for cancer treatment are known to induce cancer cell death through necrosis [6]. MRS of hyperpolarized [1,4-$^{13}C^{2}$]fumarate can play an important role in studying necrosis *in vivo* in these processes. The model presented here, turpentine injection into living tissue, provides a robust and easy to control technical validation method that causes necrosis and inflammatory response, and therefore can be useful in studying cellular death via necrosis. Turpentine is a mixture of alkylated aromatic hydrocarbons designed to dissolve fat, and thus they can effectively cause lipid dissolution.

In conclusion, we have demonstrated the feasibility of probing the dual enzymatic pathways of [1-^{13}C]pyruvate and [1,4-$^{13}C_2$]fumarate in a clinical dual PET/MR system. The *in vitro* measurements showed that the polarization values achieved for two substrates when polarized together, were comparable to the values obtained when each substrate was polarized individually. The experimental setup can be useful to investigate the ability of various hyperpolarized ^{13}C substrates and PET tracers, like ^{18}F-FDG, malate/fumarate ratio and lactate/pyruvate ratio in monitoring the response of cancer to treatment. The setup also can be used to investigate the correlation between the analogous PET and ^{13}C MRS markers. Moreover, clinical PET/MR scanners, that are becoming widely available, could contribute not only to human clinical routine examinations, but also to biomedical researches in small animals.

Acknowledgment

Adam E. Hansen is gratefully acknowledged for technical support. We would also like to acknowledge the financial support from Danish Research Council (Grant Number 1331-00259A) and the Danish National Research Foundation (Grant Number DNRF124).

Disclosure

Nothing to disclose.

References

1. Ardenkjær-Larsen JH, Fridlund B, Gram A, Hansson G, Hansson L, Lerche MH, Servin R, Thaning M, Golman K. Increase in signal-to-noise ratio of> 10,000 times in liquid-state NMR. *Proceedings of the National Academy of Sciences.* 2003;100(18):10158-10163.
2. Day SE, Kettunen MI, Gallagher FA, Hu DE, Lerche M, Wolber J, Golman K, Ardenkjaer-Larsen JH, Brindle KM. Detecting tumor response to treatment using hyperpolarized 13C magnetic resonance imaging and spectroscopy. *Nature medicine.* 2007;13(11):1382-1387.
3. Witney TH, Kettunen MI, Hu DE, Gallagher FA, Bohndiek SE, Napolitano R, Brindle KM. Detecting treatment response in a model of human breast adenocarcinoma using hyperpolarised [1-13C]pyruvate and [1,4-13C2]fumarate. *British journal of cancer.* 2010;103(9):1400-1406.
4. Kurhanewicz J, Vigneron DB, Brindle K, Chekmenev EY, Comment A, Cunningham CH, Deberardinis RJ, Green GG, Leach MO, Rajan SS, Rizi RR, Ross BD, Warren WS, Malloy CR. Analysis of cancer metabolism by imaging hyperpolarized nuclei: prospects for translation to clinical research. *Neoplasia.* 2011;13(2):81-97.
5. Albers MJ, Bok R, Chen AP, Cunningham CH, Zierhut ML, Zhang VY, Kohler SJ, Tropp J, Hurd RE, Yen YF, Nelson SJ, Vigneron DB, Kurhanewicz J. Hyperpolarized 13C lactate, pyruvate, and alanine: noninvasive biomarkers for prostate cancer detection and grading. *Cancer research.* 2008;68(20):8607-8615.
6. Gallagher FA, Kettunen MI, Hu DE, Jensen PR, Zandt RI, Karlsson M, Gisselsson A, Nelson SK, Witney TH, Bohndiek SE, Hansson G, Peitersen T, Lerche MH, Brindle KM. Production of hyperpolarized [1,4-13C2]malate from [1,4-13C2]fumarate is a marker of cell necrosis and treatment response in tumors. *Proceedings of the National Academy of Sciences of the United States of America.* 2009;106(47):19801-19806.
7. Clatworthy MR, Kettunen MI, Hu DE, Mathews RJ, Witney TH, Kennedy BW, Bohndiek SE, Gallagher FA, Jarvis LB, Smith KG, Brindle KM. Magnetic resonance imaging with hyperpolarized [1,4-(13)C2]fumarate allows detection of early renal acute tubular necrosis. *Proceedings of the National Academy of Sciences of the United States of America.* 2012;109(33):13374-13379.
8. Mignion L, Dutta P, Martinez GV, Foroutan P, Gillies RJ, Jordan BF. Monitoring Chemotherapeutic Response by Hyperpolarized 13C-Fumarate MRS and Diffusion MRI. *Cancer research.* 2014.
9. Hill DA, Hill JJ. An Investigation of Pol an" zed-Proton Target Materials by Differential Calorimetry-Preliminary Results. 1980.
10. Karlsson M, Jensen P, Duus J, Meier S, Lerche M. Development of Dissolution DNP-MR Substrates for Metabolic Research. *Appl Magn Reson.* 2012;43(1-2):223-236.
11. von Morze C, Bok RA, Reed GD, Ardenkjaer-Larsen JH, Kurhanewicz J, Vigneron DB. Simultaneous Multiagent Hyperpolarized (13)C Perfusion Imaging. *Magnetic resonance in medicine : official journal of the Society of Magnetic*

Resonance in Medicine / Society of Magnetic Resonance in Medicine. 2014;72(6):1599-1609.
12. von Morze C, Larson PE, Hu S, Yoshihara HA, Bok RA, Goga A, Ardenkjaer-Larsen JH, Vigneron DB. Investigating tumor perfusion and metabolism using multiple hyperpolarized 13 C compounds: HP001, pyruvate and urea. *Magnetic resonance imaging.* 2012;30(3):305-311.
13. Wilson DM, Keshari KR, Larson PEZ, Chen AP, Hu S, Van Criekinge M, Bok R, Nelson SJ, Macdonald JM, Vigneron DB, Kurhanewicz J. Multi-compound Polarization by DNP Allows Simultaneous Assessment of Multiple Enzymatic Activities In Vivo. *Journal of magnetic resonance (San Diego, Calif. : 1997).* 2010;205(1):141-147.
14. Witney TH, Kettunen MI, Hu De, Gallagher FA, Bohndiek SE, Napolitano R, Brindle KM. Detecting treatment response in a model of human breast adenocarcinoma using hyperpolarised [1-(13)C]pyruvate and [1,4-(13)C(2)]fumarate. *British Journal of Cancer.* 2010;103(9):1400-1406.
15. Ardenkjaer-Larsen JH, Leach AM, Clarke N, Urbahn J, Anderson D, Skloss TW. Dynamic nuclear polarization polarizer for sterile use intent. *NMR in biomedicine.* 2011;24(8):927-932.
16. Malinowski RM, Lipsø KW, Lerche MH, Ardenkjær-Larsen JH. Dissolution Dynamic Nuclear Polarization capability study with fluid path. *Journal of Magnetic Resonance.* 2016.
17. Park I, Larson PE, Tropp JL, Carvajal L, Reed G, Bok R, Robb F, Bringas J, Kells A, Pivirotto P. Dynamic hyperpolarized carbon-13 MR metabolic imaging of nonhuman primate brain. *Magnetic Resonance in Medicine.* 2014;71(1):19-25.
18. Hanahan D, Weinberg RA. Hallmarks of cancer: the next generation. *Cell.* 2011;144(5):646-674.
19. Brindle K. New approaches for imaging tumour responses to treatment. *Nature reviews. Cancer.* 2008;8(2):94-107.
20. Bohndiek SE, Kettunen MI, Hu DE, Witney TH, Kennedy BW, Gallagher FA, Brindle KM. Detection of tumor response to a vascular disrupting agent by hyperpolarized 13C magnetic resonance spectroscopy. *Mol Cancer Ther.* 2010;9(12):3278-3288.
21. Nielsen PM, Eldirdiri A, Bertelsen LB, Jørgensen HS, Ardenkjaer-Larsen JH, Laustsen C. Fumarase activity: an in vivo and in vitro biomarker for acute kidney injury. *Scientific Reports.* 2017;7:40812.
22. Chan FK-M, Moriwaki K, De Rosa MJ. Detection of necrosis by release of lactate dehydrogenase activity. *Immune Homeostasis: Methods and Protocols.* 2013:65-70.
23. Grivennikov SI, Greten FR, Karin M. Immunity, inflammation, and cancer. *Cell.* 2010;140(6):883-899.
24. De Visser KE, Eichten A, Coussens LM. Paradoxical roles of the immune system during cancer development. *Nature reviews cancer.* 2006;6(1):24-37.
25. Gutte H, Hansen AE, Henriksen ST, Johannesen HH, Ardenkjaer-Larsen J, Vignaud A, Hansen AE, Børresen B, Klausen TL, Wittekind A-MN. Simultaneous hyperpolarized 13C-pyruvate MRI and 18F-FDG-PET in cancer (hyperPET):

feasibility of a new imaging concept using a clinical PET/MRI scanner. *American journal of nuclear medicine and molecular imaging.* 2015;5(1):38.
26. Gutte H, Hansen AE, Larsen M, Rahbek S, Henriksen S, Johannesen H, Ardenkjær-Larsen J, Kristensen A, Højgaard L, Kjær A. Simultaneous hyperpolarized 13C-pyruvate MRI and 18F-FDG-PET (hyperPET) in 10 canine cancer patients. *Journal of Nuclear Medicine.* 2015:jnumed. 115.156364.
27. Akiyama H, Barger S, Barnum S, Bradt B, Bauer J, Cole GM, Cooper NR, Eikelenboom P, Emmerling M, Fiebich BL. Inflammation and Alzheimer's disease. *Neurobiology of aging.* 2000;21(3):383-421.
28. Cosi C, Suzuki H, Milani D, Facci L, Menegazzi M, Vantini G, Kanai Y, Skaper S. Poly (ADP-ribose) polymerase: Early involvement in glutamate-induced neurotoxicity in cultured cerebellar granule cells. *Journal of neuroscience research.* 1994;39(1):38-46.
29. Brennan MA, Cookson BT. Salmonella induces macrophage death by caspase-1-dependent necrosis. *Molecular microbiology.* 2000;38(1):31-40.
30. Lenardo MJ, Angleman SB, Bounkeua V, Dimas J, Duvall MG, Graubard MB, Hornung F, Selkirk MC, Speirs CK, Trageser C. Cytopathic killing of peripheral blood CD4+ T lymphocytes by human immunodeficiency virus type 1 appears necrotic rather than apoptotic and does not require env. *Journal of virology.* 2002;76(10):5082-5093.
31. Murdoch W, Wilken C, Young D. Sequence of apoptosis and inflammatory necrosis within the formative ovulatory site of sheep follicles. *Journal of reproduction and fertility.* 1999;117(2):325-329.
32. Chautan M, Chazal G, Cecconi F, Gruss P, Golstein P. Interdigital cell death can occur through a necrotic and caspase-independent pathway. *Current biology.* 1999;9(17):967-S961.

Figure legends

Figure 1

(a) The fluid path that goes into the SPINlab. The fluid path consists of a syringe that contains the DM and sample vial that contains the ^{13}C substrate to be polarized. The two are connected by two concentric tubes. During the dissolution the DM is transferred through the inner tube to the sample vial, where it dissolves the hyperpolarized substrate. The dissolved material flows back through the outer tube lumen toward the syringe and out of the SPINlab via the exit tube. (b) shows schematic draw of the sample vial. The vial is prepared by first adding the PA and then freezing it in LN_2 and then adding the FA. The vial is then kept in LN_2 during the rest of preparation of the fluid path to attain two separate layers in the vial. (c) shows the path of the vial once it is inserted in the SPINlab. The vial is initially placed in the airlock for 20 min to allow the sample to melt. Then, it is lowered in multiple steps, back and forth, along the path, to avoid excessive increase in temperature at the sample pot until it settles at the sample pot.

Figure 2

Typical polarization curve (shown with solid lines) starting from time = 0. The dashed and dash-dotted curves in the figure shows the temperature recorded at two positions in the SPINlab, which are the sample pot and the equilibrator, respectively. Before the start of the polarization build-up is the period during which the lowering process takes place. In (a) where multi-steps lowering is used, the variation in temperature at the equilibrator level is smaller compared with (b) where only two lowering steps were used. At the sample pot, the temperature stays almost constant for multi-steps lowering, while for the two-step

lowering there is a rise in temperature for some time (about 25 minutes) before the temperature settles at 0.8 K.

Figure 3

The expected positions of the peaks of interest following the administration of FA and PA. The figure illustrates that the ^{13}C spectrum is sparse allowing co-polarization and simultaneous imaging of [1,4-$^{13}C_2$]fumarate and [1-^{13}C]pyruvate.

Figure 4

The anatomical axial image of the first rat (a) acquired at the location of the necrotic tissue. The image was acquired with turbo spin echo (TR= 5.7 s, TE= 84 ms, echo train length of 18, number of phase encoding steps 234, Number of averages of 5, final matrix size of 256x256 covering a FOV of 100 mm x 100 mm with slice thickness of 2 mm). (b) shows the spectrum at the necrotic tissue with the fumarate peak and the malate doublet. Clear malate signal can be observed in the spectrum. The small peak at the right of the spectrum at 165 ppm is due to fold over of the ^{13}C-urea phantom. (c) and (d) shows the metabolic maps of fumarate and malate, respectively. Notice that the malate production is confined to the necrotic region. (e) shows an axial slice with 12 mm thickness (sum of 6 adjacent slices) with the FDG uptake in a plane containing the necrotic tissue.

Figure 5

The anatomical axial image of the second rat (a) acquired at the location of the necrotic tissue. The proton image was acquired similar to Figure 4-a. A coronal maximum intensity projection image which shows the FDG uptake by the different organs is illustrated in (b). (c) shows an axial slice with 12 mm thickness (sum of 6 adjacent slices) with the FDG

uptake in a plane containing the necrotic tissue. (d) and (e) show the phased real part spectra at the necrotic tissue, the blue box in (a), acquired for single injection of FA and dual injection of FA and PA, respectively. The malate signal can be seen in both spectra. In dual FA and PA experiment additional peaks are observed for lactate, alanine, pyruvate-hydrate and bicarbonate. Some ringing due to truncation is observed (80 ms acquisition time with apodization) (f to i) shows the metabolic maps of pyruvate, lactate, fumarate and malate, respectively.

Tables

Table 1: Solid state DNP build-up data for three different samples with two different loading profiles

Concentrations (FA/AH111501)	2.8 M/15 mM		3.6 M/8 mM		3.6 M/12 mM	
No. insertion steps	ONE	TWO	ONE	TWO	ONE	TWO
Build-up time constant (s)	9448	5913	6718	6765	2725	3659
S(t=∞) (a.u.)	1311	1054	740	1140	969	993
Liquid-state polarization(%)	39		38		37	

Table 2: Liquid state polarization and T_1 measurements for the sample with FA (3.6 M) with 8 mM of AH111501 radical

n=5	Fumarate		Pyruvate
	Dual	Single	Dual
T_1 (s)	57±2	58±2	70±3
Polarization (%)	35±5	37±6	37±6

561 **Figure 1:**

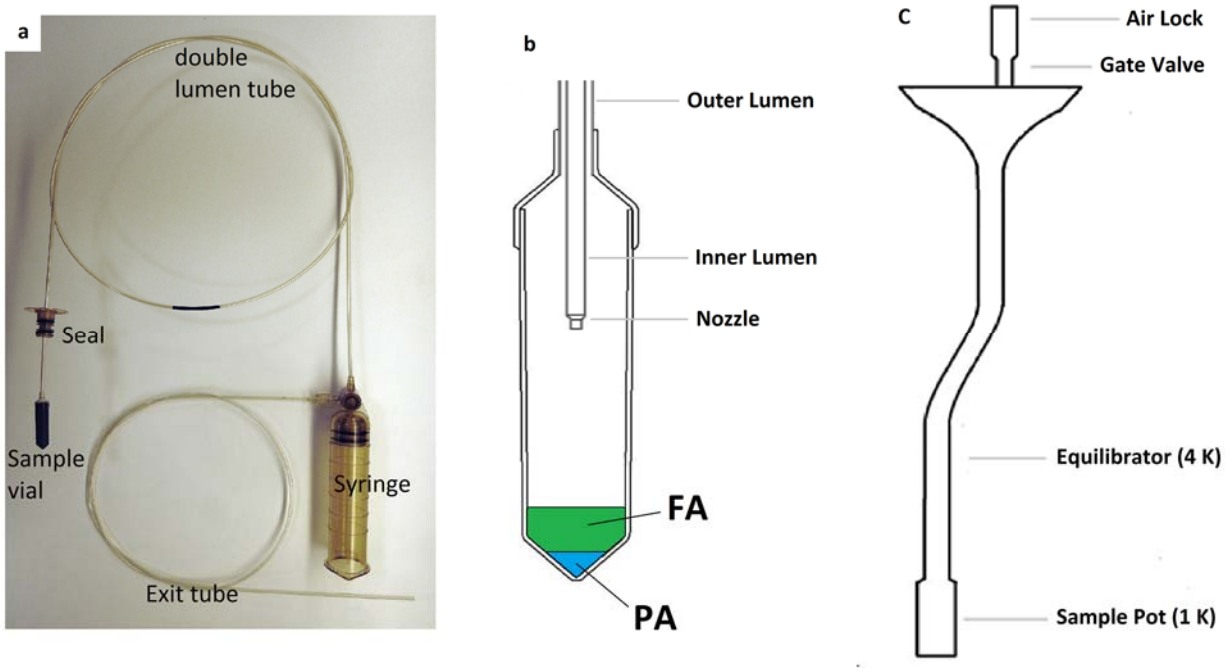

562

563

564 **Figure 2:**

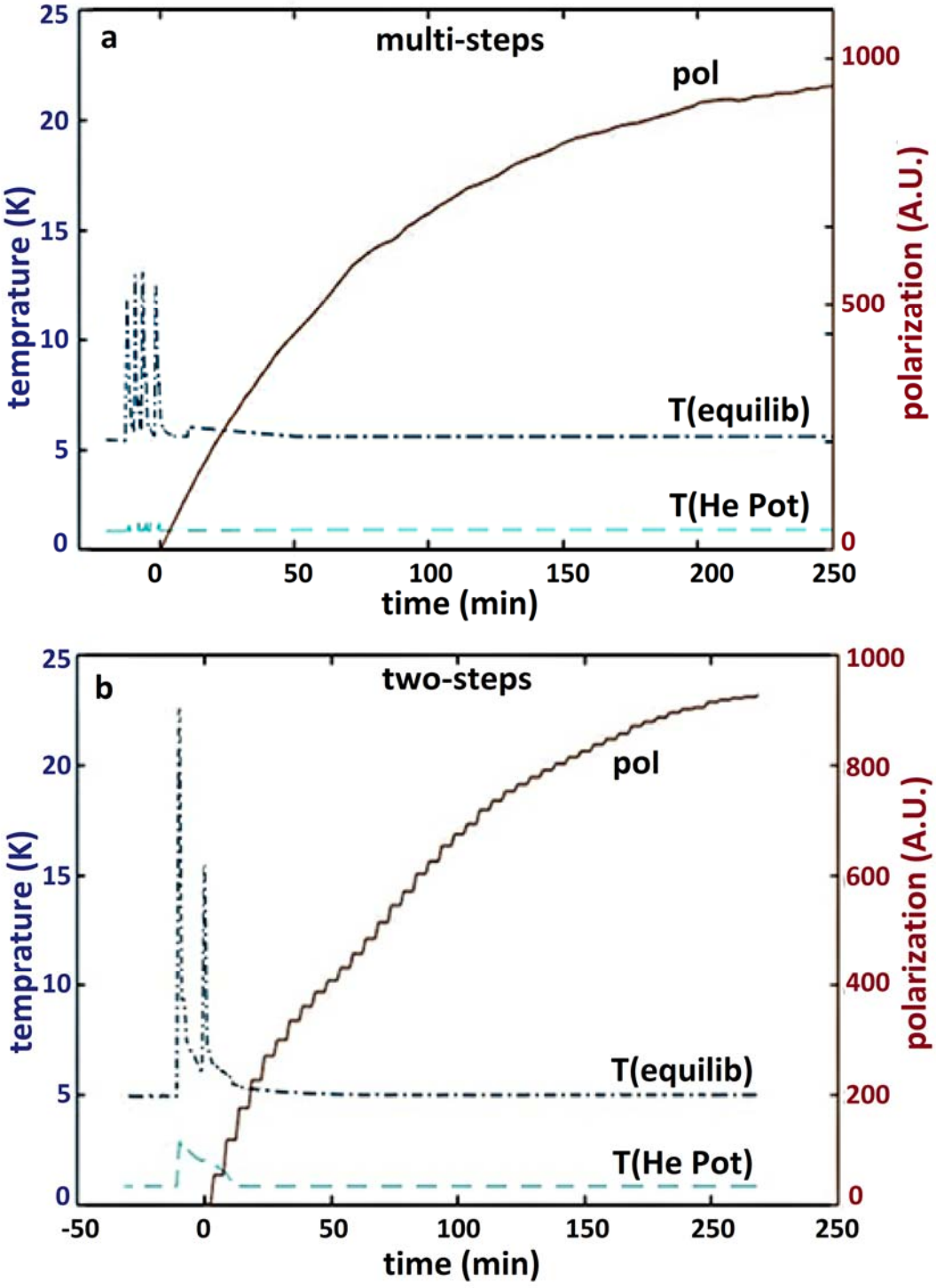

565

566

Figure 3:

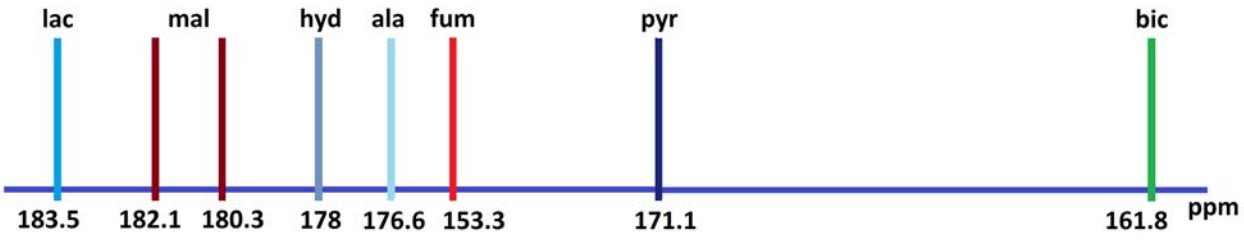
lac
mal
hyd
ala
fum
pyr
bic
183.5
182.1
180.3
178
176.6
153.3
171.1
161.8
ppm

570 **Figure 4:**

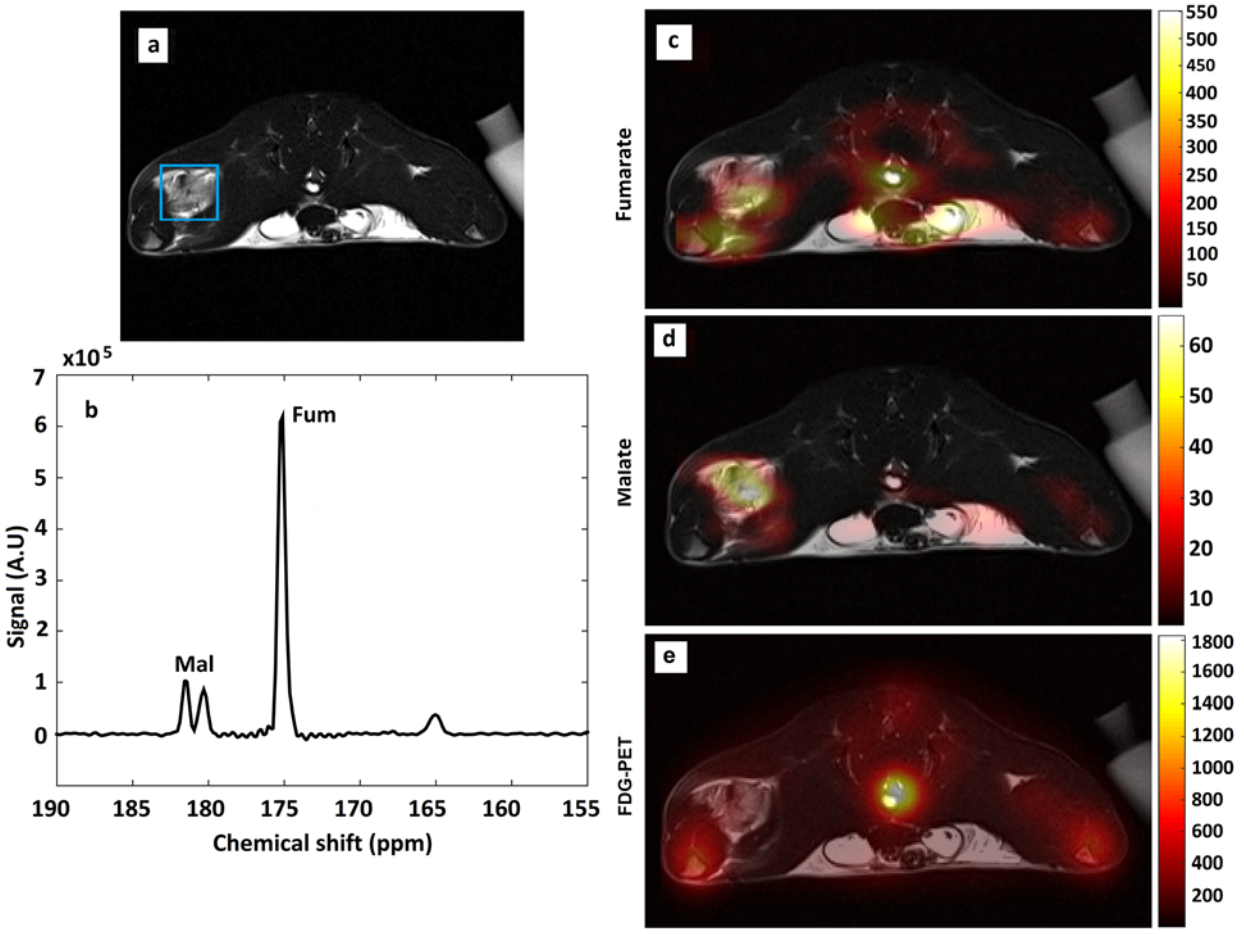

571

572

573 **Figure 5:**

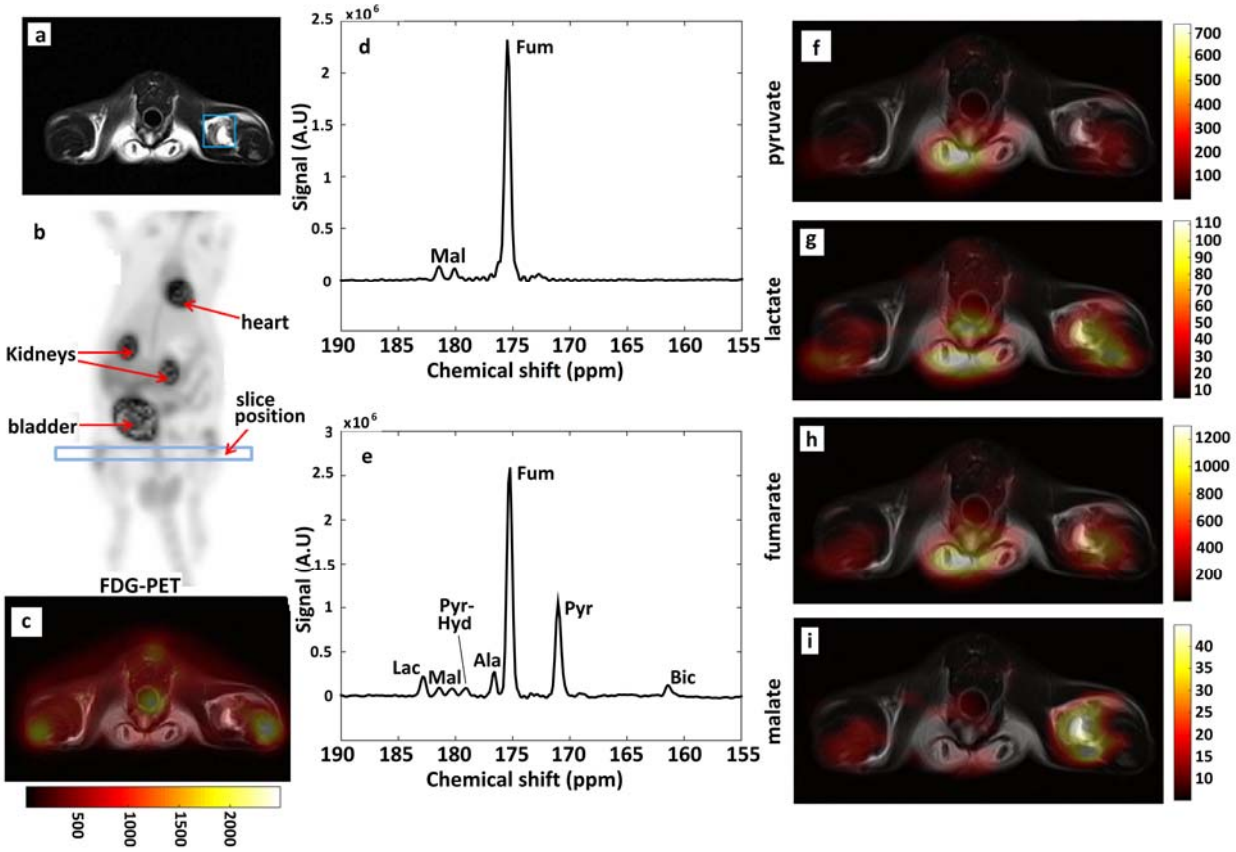

574